NRC·CNRC

NRC Publications Archive
Archives des publications du CNRC

Imaging the Kramers-Henneberger atom

Morales, Felipe; Richter, Maria; Patchkovskii, Serguei; Smirnova, Olga

This publication could be one of several versions: author's original, accepted manuscript or the publisher's version. / La version de cette publication peut être l'une des suivantes : la version prépublication de l'auteur, la version acceptée du manuscrit ou la version de l'éditeur.
For the publisher's version, please access the DOI link below./ Pour consulter la version de l'éditeur, utilisez le lien DOI ci-dessous.

Publisher's version / Version de l'éditeur:
https://doi.org/10.1073/pnas.1105916108
Proceedings of the National Academy of Sciences, 108, 41, pp. 16906-16911, 2011-09-19

NRC Publications Record / Notice d'Archives des publications de CNRC:
https://nrc-publications.canada.ca/eng/view/object/?id=6c193677-0f3d-488a-ab2d-d87dcceb4550
https://publications-cnrc.canada.ca/fra/voir/objet/?id=6c193677-0f3d-488a-ab2d-d87dcceb4550

Access and use of this website and the material on it are subject to the Terms and Conditions set forth at https://nrc-publications.canada.ca/eng/copyright
READ THESE TERMS AND CONDITIONS CAREFULLY BEFORE USING THIS WEBSITE.

L'accès à ce site Web et l'utilisation de son contenu sont assujettis aux conditions présentées dans le site https://publications-cnrc.canada.ca/fra/droits
LISEZ CES CONDITIONS ATTENTIVEMENT AVANT D'UTILISER CE SITE WEB.

Questions? Contact the NRC Publications Archive team at PublicationsArchive-ArchivesPublications@nrc-cnrc.gc.ca. If you wish to email the authors directly, please see the first page of the publication for their contact information.

Vous avez des questions? Nous pouvons vous aider. Pour communiquer directement avec un auteur, consultez la première page de la revue dans laquelle son article a été publié afin de trouver ses coordonnées. Si vous n'arrivez pas à les repérer, communiquez avec nous à PublicationsArchive-ArchivesPublications@nrc-cnrc.gc.ca.

National Research Council Canada | Conseil national de recherches Canada

Canada

Imaging the Kramers–Henneberger atom

Felipe Morales[1], Maria Richter[1], Serguei Patchkovskii[2], and Olga Smirnova[3]

[a]Max-Born Institute for Nonlinear Optics, Max-Born-Strasse 2A, D-12489 Berlin, Germany

Edited* by Paul B. Corkum, University of Ottawa, Ottawa, Canada, and approved July 25, 2011 (received for review April 14, 2011)

Today laser pulses with electric fields comparable to or higher than the electrostatic forces binding valence electrons in atoms and molecules have become a routine tool with applications in laser acceleration of electrons and ions, generation of short wavelength emission from plasmas and clusters, laser fusion, etc. Intense fields are also naturally created during laser filamentation in the air or due to local field enhancements in the vicinity of metal nanoparticles. One would expect that very intense fields would always lead to fast ionization of atoms or molecules. However, recently observed acceleration of neutral atoms [Eichmann et al. (2009) *Nature* 461:1261–1264] at the rate of 10^{15} m/s^2 when exposed to very intense IR laser pulses demonstrated that substantial fraction of atoms remained stable during the pulse. Here we show that the electronic structure of these stable "laser-dressed" atoms can be directly imaged by photoelectron spectroscopy. Our findings open the way to visualizing and controlling bound electron dynamics in strong laser fields and reexamining its role in various strong-field processes, including microscopic description of high order Kerr nonlinearities and their role in laser filamentation [Béjot et al. (2010) *Phys Rev Lett* 104:103903].

dressed atom | atomic stabilization | strong-field ionization | Kramers–Henneberger approximation

One of the most beautiful theoretical concepts of strong-field physics defies common intuition, which suggests that strong laser fields would always ionize atomic systems faster than weak fields, and argues in favor of the opposite effect—the atomic stabilization (1–4). Stabilization means that the ionization probability of the atom or molecule does not increase or even decreases with increasing the laser field intensity. The essence of the phenomenon is that the strong laser field and the Coulomb force work together to create a new effective binding potential. The new system—the laser-dressed atom—is stable against ionization. With the same principle, one can use strong laser fields to bind same-sign charges and create a "molecule without electrons" (5). To get an idea about the origin and the shape of the effective binding potential for the electron in a superatomic field, recall that such field completely suppresses the potential barrier that normally confines the bound electron (Fig. 1*A*). Now the electron can very quickly leave the atom and become almost free: Its motion is dominated by the oscillations in the laser field and its interaction with the ion is weak (Fig. 1*B*). To take this weak interaction into account, it is convenient to move into the reference frame associated with the oscillating electron. The ion's potential seen from the electron's reference frame *and averaged over its oscillations* is called the Kramers–Henneberger (KH) potential (6). The averaged potential well, although distinctly different from the original atomic potential, is indeed capable of supporting infinitely many bound states of the KH atom (Fig. 1*C*). But should one believe this concept, borne out of the frame transformation?

Indeed, the new states are stable and physically relevant only if all the harmonics of the oscillating ionic potential—the terms which were zero on average—can be neglected. Although averaging over fast oscillations appears to be natural for sufficiently high frequencies in the extreme ultraviolet (XUV) range (see, e.g., refs. 7–9 for vacuum ultraviolet), typical of the new generation of light sources, the extension to the low frequency IR laser fields is not intuitive, with conflicting theoretical and mathematical arguments in favor (10–13) and against it (14, 15).

Although the concept of stabilization and of the KH atom stimulated a lot of research about two decades ago (see, e.g., ref. 16 and references therein), so far the KH atom has existed only in the realm of theory. The lack of convincing experimental evidence has gradually quenched the theoretical activity. The whole story could have probably been forgotten by now if it were not for the circumstantial and seemingly disconnected experimental evidence obtained very recently. The most striking example is the experiment (17) reporting unprecedented acceleration of neutral atoms subjected to superstrong IR laser fields, at a rate of 10^{15} m/s^2. This experiment, albeit indirectly, demonstrates the existence of stable atoms in superstrong IR fields. Another example is offered by paradigm-shifting results on the filamentation of ultrashort IR femtosecond laser pulses in the air without substantial plasma formation (18), which implies surprising and unexpected stability of small molecules in the intense fields of the filament. The recent body of experimental data has prompted us to ask the following question: Is it possible to directly visualize the exotic electronic structure of the KH atom or molecule with a typical modern-day experimental setup? We show that not only is the KH atom a physically relevant object in strong IR fields, but also that its electronic structure can be unambiguously identified in the angle resolved photoelectron spectra obtained with standard femtosecond lasers and velocity map imaging techniques (19). Most remarkably, we find that the KH-atom is formed and can be detected even before the onset of stabilization. Our analysis is done for an alkaline atom (potassium), where the required parameters are similar to those in recent experiments (20, 21).

The Kramers–Henneberger Atom

To introduce the KH atom formally, consider the time-dependent Schrödinger equation (TDSE) describing the electron interacting with the core potential $U_{\rm ion}(\mathbf{r})$ and the laser field $\mathbf{E}(t)$:

$$i\partial\Psi/\partial t = [-\nabla^2/2 + U_{\rm ion}(\mathbf{r}) + \mathbf{E}(t)\mathbf{r}]\Psi. \quad [1]$$

This equation can be rewritten in the oscillating reference frame with the help of well-known unitary transformation (see, e.g., ref. 22), which is a quantum mechanical equivalent of the classical variable substitution $\mathbf{r}_{\rm KH} = \mathbf{r} - \alpha(t)\mathbf{e}_z$,

$$i\partial\Psi_{\rm KH}/\partial t = [-\nabla^2/2 + U_{\rm ion}(\mathbf{r}_{\rm KH} + \alpha(t)\mathbf{e}_z)]\Psi_{\rm KH}. \quad [2]$$

Here $\alpha(t) = \alpha_0\cos(\omega t)$ describes the electron oscillations with amplitude $\alpha_0 = E/\omega^2$ in the field $\mathbf{E}(t) = \mathbf{e}_z E\cos(\omega t)$, linearly polarized along the z axis (unit vector $\mathbf{e}_z$). One can always split

Author contributions: O.S. designed research; F.M., M.R., and S.P. performed research; F.M., M.R., S.P., and O.S. analyzed data; and S.P. and O.S. wrote the paper.

The authors declare no conflict of interest.

*This Direct Submission article had a prearranged editor.

Freely available online through the PNAS open access option.

[1]F.M. and M.R. contributed equally to this work.

[2]On leave from: National Research Council of Canada, 100 Sussex Drive, Ottawa, ON, Canada K1A 0R6.

[3]To whom correspondence should be addressed. E-mail: smirnova@mbi-berlin.de.

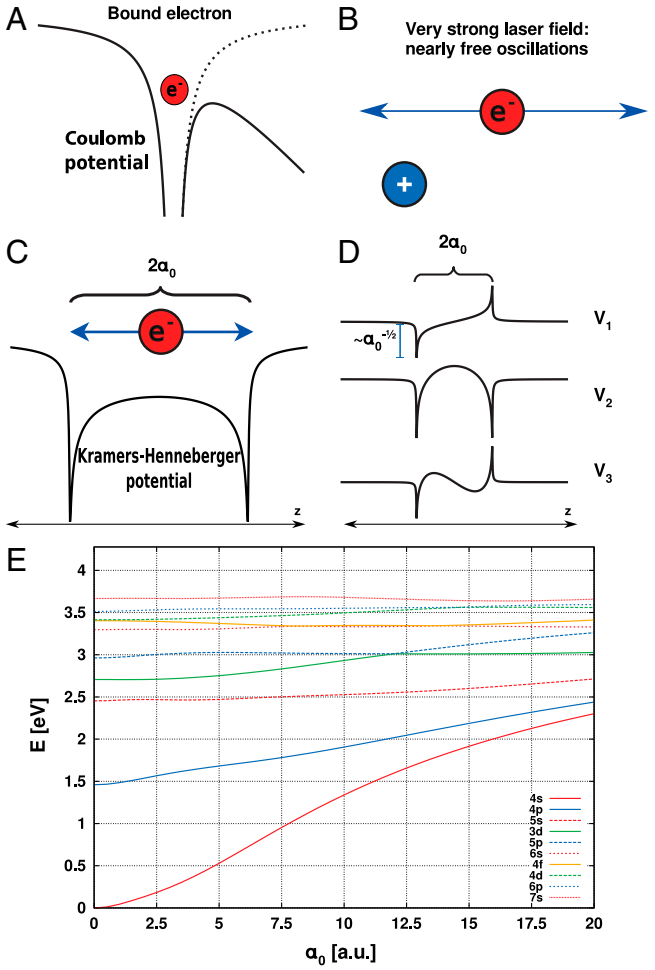

Fig. 1. The Kramers–Henneberger atom. (*A*) The binding potential well without (dashed line) and with (solid line) external superatomic electric field. (*B*) In the superatomic field the electron becomes almost free and its motion is dominated by the oscillations in the field with the amplitude $\alpha_0 = E/\omega^2$, where E and ω are the laser field strength and frequency, respectively. (*C*) The sketch of the Kramers–Henneberger potential and (*D*) its harmonics. The coordinate dependence of the KH potential V_0 and its harmonics V_1, V_2, V_3 is shown for a one-dimensional cut through the K nucleus, along the laser polarization direction. (*E*) The energies of the Kramers–Henneberger potassium atom vs. amplitude of oscillations α_0.

the oscillating ion's potential in Eq. **2** into a time-dependent and a time-independent part:

$$U_{\text{ion}}(\mathbf{r}_{\text{KH}} + \alpha(t)\mathbf{e}_z) = V_0(\mathbf{r}_{\text{KH}}) + \sum_{n=1}^{\infty} V_n(\mathbf{r}_{\text{KH}})\cos(n\omega t), \qquad [3]$$

$$V_n(\mathbf{r}_{\text{KH}}) = \frac{1}{2\pi}\int_0^{2\pi} U_{\text{ion}}(\mathbf{r}_{\text{KH}} + \alpha_0\cos(\varphi)\mathbf{e}_z)\cos(n\varphi)d\varphi, \qquad [4]$$

where $V_0(\mathbf{r}_{\text{KH}})$ is the KH potential and $V_n(\mathbf{r}_{\text{KH}})$ $(n \neq 0)$ are the harmonics of the oscillating ion's potential (schematically shown in Fig. 1*D*; see also ref. 23), responsible for the ionization and distortion of the KH atom. However, Eq. **3** does not imply that the bound states of the KH potential $V_0(\mathbf{r}_{\text{KH}})$ are physically relevant, because the rest of the terms in Eq. **3** cannot be always omitted. For example, the well-known Autler–Townes splitting of the resonantly driven bound states cannot be described by the KH potential $[V_0(\mathbf{r}_{\text{KH}})]$ alone. Another textbook example —the negative Stark shift of the ground state of an atom in a low frequency field—also contrasts the always positive ground state shift in the KH potential (see Fig. 1*E*). Thus, several important questions arise: When do the KH states become physically relevant and can be directly visualized? Do the KH states become physically relevant only after the onset of the stabilization or is the stabilization not required? Can angular-resolved photoelectron spectra recorded in strong laser fields provide information about the spatial structure of these bound states?

In conventional photoelectron spectroscopy, the direct correspondence between the initial bound and the final continuum electron states is derived from the energy conservation, which is helpful only if the number of absorbed photons is fixed and known. This is usually the case for weak fields. In strong fields of short laser pulses different multiphoton pathways can lead to the same final energy; bound and continuum states are significantly broadened and shifted, making identification of spectral lines challenging, if not hopeless. This is especially true in the intense low frequency field regime (24), where different multiphoton peaks often merge and the photoelectron spectrum becomes nearly continuous. However, the conventional spectroscopic approach may be recovered with the onset of the KH regime: If the harmonics of the oscillating potential responsible for ionization of the KH atom indeed become small, the levels of the KH atom and the spatial structure will be faithfully reproduced in the photoelectron spectra. However, because the emergence of the KH atom is expected at high field strength, significant ionization may already occur before the onset of this regime, leading to contamination of the useful photoelectron signal. Had the KH atom existed, this contamination could have completely hidden it from the experimental observation.

Results

We have chosen to look at the potassium atom interacting with a typical femtosecond laser pulse with 800-nm wavelength. The potassium ionization potential is only $I_p = 4.34$ eV and hence the superatomic intensity, which suppresses the binding potential barrier below the ground state energy (Fig. 1*A*), is only $I_{\text{BS}} \simeq 10^{12}$ W/cm^2 (BS stands for "barrier suppression"). Thus, one can easily probe this atom experimentally at intensities several orders of magnitude higher than I_{BS}. Because the 800-nm laser field is nearly resonant with the 4*s*-4*p* transition, the first significant modification of the bound states is related to the Autler–Townes splitting, clearly observed in the angular-resolved photoelectron spectra of potassium in the experiment (25). Here we look at much higher intensities. We first solved the TDSE Eq. **1** to obtain the potassium photoelectron spectra for a 800-nm laser pulse with intensity $I = 1.4 \times 10^{13}$ W/cm^2, one order of magnitude higher than I_{BS}. The laser pulse was smoothly turned on in six laser cycles to reach its peak intensity, which remained constant for the next 13 cycles followed by a smooth six cycle turn-off. The total duration of this "flat-top" pulse was 65 fs. Details of the calculation are given in *Methods*. Although the distinct spectral lines (rings) are clearly visible in the angle-resolved spectra in Fig. 2*A*, these lines cannot be directly associated with the potassium bound states by analyzing the symmetry of both the final continuum state and the initial bound state, their respective energies, and the number of absorbed photons. Are the KH states relevant for these spectra? To check this idea, we first found the eigenenergies and eigenstates of the KH atom (i.e., of the potential V_0). Next, we solve the TDSE in the KH frame, Eq. **2**, starting with the KH atom already prepared in one of its eigenstates and smoothly turning on just a few harmonics V_n (typically V_1 and V_2). (Further details can be found in *Methods*.) If all harmonics $V_n(t)$ are strong, none of them can be neglected and the separation in Eq. **3** is neither relevant nor beneficial; converged results will not be achieved unless all harmonics are included in the calculation.

Ionization of the KH atom by the KH harmonics leads to the photoelectron spectra shown in Fig. 2 *B* and *C*. Because of the 4*s*-4*p* resonance we expect significant population of KH-4p state before the onset of the KH regime. Therefore, we show photoelectron spectra resulting from ionization of the KH atom

PHYSICS

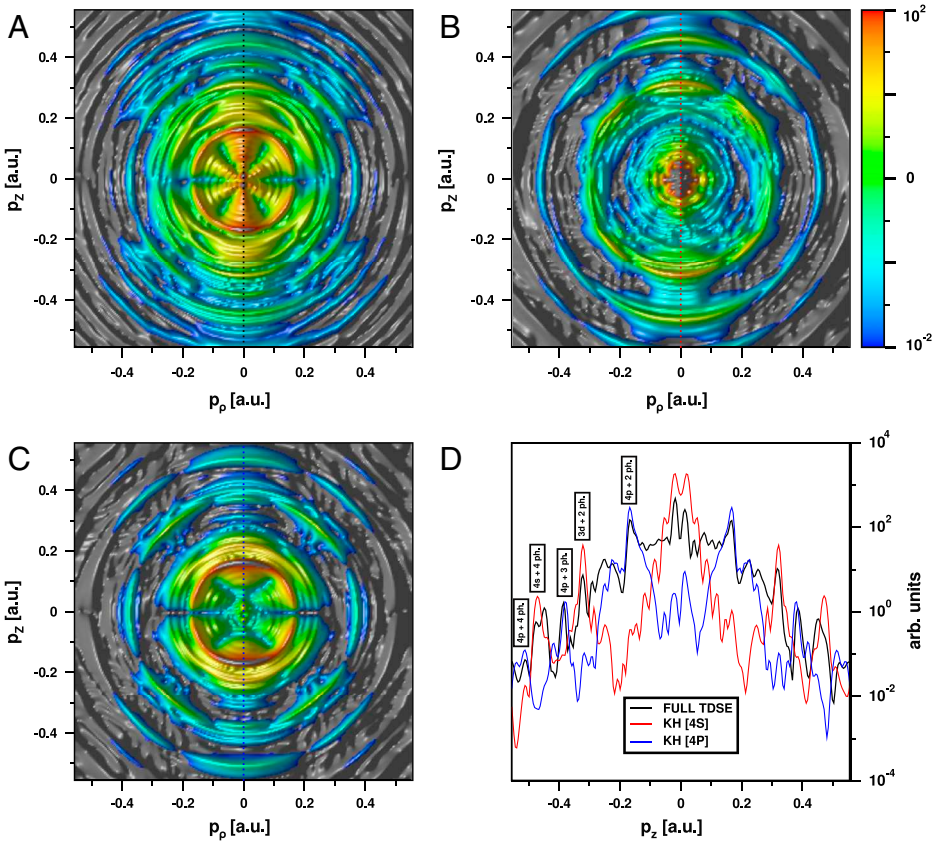

Fig. 2. Direct visualization of the KH atom in the photoelectron spectra. p_z and p_ρ are electron momenta along and perpendicular to the laser field, correspondingly. The photoelectron spectra correspond to a section of the three-dimensional photoelectron momentum distribution with the out-of-plane momentum being zero. (*A*) Angle and energy-resolved photoelectron spectrum for potassium interacting with 800 nm, 1.4×10^{13} W/cm^2, 65-fs laser pulse. (*B*) The photoelectron spectrum resulting from ionization of the KH potassium atom, initially prepared in the KH state 4*s* and probed by the harmonics V_1-V_5. The laser parameters are $\lambda = 800$ nm, intensity 1.4×10^{13} W/cm^2. (*C*) Same as *B*, but for the KH atom initially prepared in the KH state 4*p*. (*D*) Comparison of ab initio photoelectron spectrum (black solid line) and spectrum resulting from the ionization of the KH atom initially prepared in the states 4*s* (red line) and 4*p* (blue line) for electrons ejected along the laser field. The most prominent lines in this spectrum are assigned based on the symmetries of KH-bound states and net number of absorbed photons (e.g., net two-photon absorption from the initial 4*p* KH state gives rise to the spectral line observed near $|p| = 0.2$ a.u.). A strong signal coming from the 3*d* KH state is due to the two-photon population from the initial 4*s* KH state during the turn-on of the KH harmonics.

initially prepared in the KH states 4*s* (Fig. 2*B*) and 4*p* (Fig. 2*C*). The first harmonic V_1 is quite significant and leads to "multiphoton processes," including "wave mixing" between V_1 and other harmonics (it was sufficient to include harmonics V_2–V_5). However even in this case, all the spectral lines in Fig. 2 *B* and *C* can be linked to the KH-bound states with a well-defined net number of photons absorbed. The essential argument in assigning the various lines is the symmetry of the initial bound and the final continuum states, which is accessible only with the angle-resolved spectra. The comparison of Fig. 2*A* with *B* and *C* shows that virtually all lines in the ab initio spectra have their twins in the photoelectron spectra of the KH atom. More detailed comparison is shown in Fig. 2*D* for electrons ejected along the laser polarization. It reveals remarkable agreement between the ab initio photoelectron spectra and the approximate KH spectra, which are explicitly relying on the existence of the KH atom and are uniquely linked to its bound states. We have assigned the prominent lines in the spectrum; see Fig. 2*D*. A strong signal coming from the 3D KH state is due to the two-photon population from the initial 4s KH state during the turn-on of the KH harmonics. Thus, at 1.4×10^{13} W/cm^2 the KH atom is already formed and can be directly seen in the photoelectron spectra; however, we do not expect stabilization for this intensity because the first harmonic V_1 is not small.

Indeed, Fig. 3 shows the survival probability $W_s = 1 - W_i$ vs. intensity for a 65-fs, 800-nm, flat-top laser pulse. Beyond $I = 2 \times 10^{13}$ W/cm^2 the ionization probability W_i does not increase with the intensity, indicating the onset of the stabilization regime. In the "stabilization plateau" the atom is left in a multitude of Rydberg states after the end of the pulse. It points to the complex physics of stabilization, which is likely to involve both known mechanisms, the adiabatic KH-type stabilization (2), and the interference stabilization (3, 4), rather than only one of them.

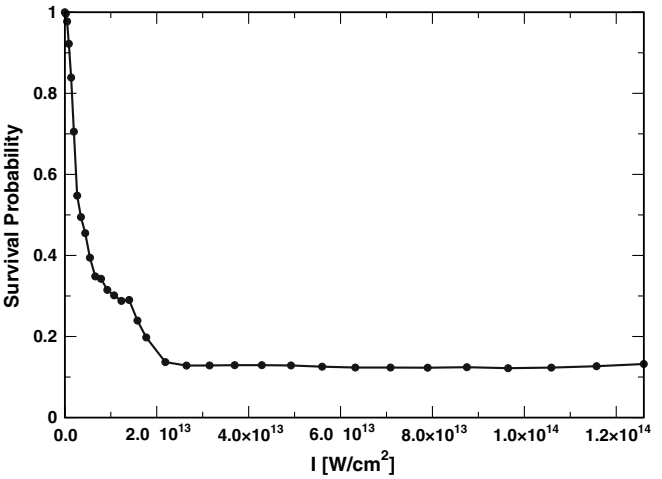

Fig. 3. Stabilization of the potassium atom in a superatomic field: survival probability vs. laser intensity for a 800 nm, 65-fs laser pulse.

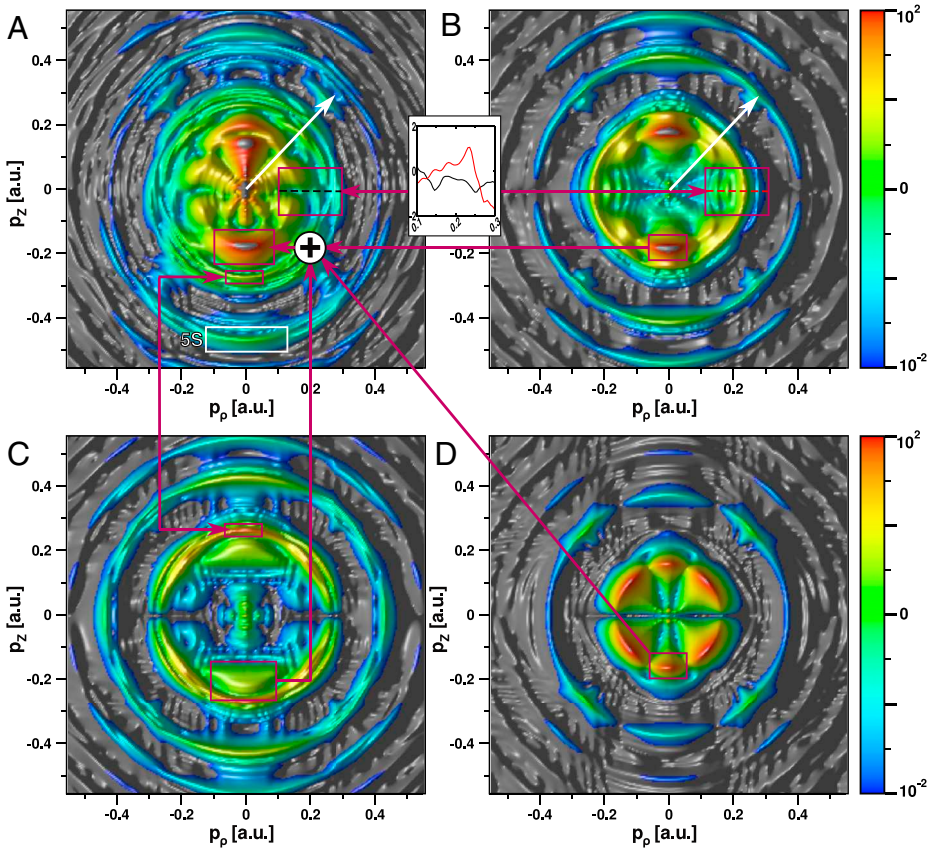

Fig. 4. Photoelectron spectroscopy of the KH potassium atom in superatomic laser fields. p_z and p_ρ are electron momenta along and perpendicular to the laser field, correspondingly. The photoelectron spectra correspond to a section of the three-dimensional photoelectron momentum distribution with the out-of-plane momentum being zero. (*A*) Angle and energy-resolved photoelectron spectrum for potassium in a 800 nm, 5.6×10^{13} W/cm^2, 65-fs laser pulse. The photoelectron images of the KH states are marked in the spectrum. (*B*) The photoelectron spectrum resulting from ionization of the KH atom initially prepared in the KH state 4*s*, probed by the harmonics V_1 and V_2 only. (*C*) Same as *B* but for the KH atom initially prepared in the KH state 4*p*. (*D*) Same as *B* but for the KH atom initially prepared in the KH state 3*d*. The white frame in *A* marks the contribution coming from the initial 5*s* state.

Is it also possible to observe the signatures of the KH atom in the stabilization regime? Indeed, after the onset of stabilization the ionization probability is low and the photoelectron spectrum could be dominated by the ionization events, which have occurred at lower intensities during the pulse turn-on. Fig. 4*A* shows potassium photoelectron spectra for a 5.6×10^{13} W/cm^2, 800-nm, flat-top pulse. Note that in the conventional strong-field ionization the maximum in the photoelectron spectrum would generally shift to lower energies as the ionization threshold increases by the ponderomotive energy $U_p = E^2/4\omega^2$ (about 3.2 eV for the current conditions). An opposite effect would occur for the KH atom, where the ionization threshold decreases and the photoelectron peaks would shift to higher energies at higher intensities (see Fig. 1*E*). Both trends can be seen in Fig. 4*A*: The low energy part of the spectrum (electron momenta $|p| < 0.14$ a.u.) is dominated by the signal coming from the relatively low laser intensities, where the KH atom is not formed yet. The size of this ring is determined by the ionization threshold for the KH atom—the continuum states within this ring cannot be populated in the KH picture.[†] Outside this ring, the spectrum is in good agreement with the KH spectra shown in Fig. 4 *B–D*, corresponding to the ionization of the KH atom initially prepared in the KH states 4*s*, 4*p*, 3*d*, and 5*s*. Only KH harmonics V_1 and V_2 are included in this calculation. One of the most striking features corresponding to the high intensity regime is the appearance of a strong photoelectron signal at 90° (see Fig. 4*B*). This signal results from "one-photon" ionization of 4*f* and 6*p* KH states populated due to bound–bound transitions between different KH states induced by the KH harmonics V_1 and V_2. Our calculations show that absorption of one net photon from 6*p* KH state leads to the g wave in the continuum. This result indicates strong modification of the KH states at these intensities as the KH atom is stretched along the polarization direction of the laser field (see Fig. 1*C*). The modification results in admixture of high angular momentum components to the KH-bound states (e.g., 6*p* KH state can get admixture of f angular momentum components) and thus changes the angular distributions of the photoelectrons for the same net number of photons absorbed during bound-continuum transitions from the KH states.[‡] Importantly, the initial population of the KH states is very sensitive to the temporal shape of the laser pulse. Our calculations reveal that the relative population of the ground 4*s* KH state strongly decreases for the Gaussian pulse of the same intensity and 20 fs duration full width half maximum.

[†]For laser parameters used in Fig. 4 $\alpha_0 = 12.5$ a.u., all KH harmonics are small and can be treated perturbatively. For the initial 4 s KH state (see Fig 1*E*), the first open ionization channel corresponds to a (net) two-photon transition, leading to photoelectrons with momentum $|p| = 0.18$ a.u. For the 4*p* and 5*s* initial states, the first open channel is also (net) two-photon, leading to $|p| = 0.25$ a.u. and $|p| = 0.31$ a.u., respectively. Finally, for the 3*d* initial state, (net) one-photon channel opens, leading to photoelectrons with momentum $|p| = 0.14$ a.u. All other initial KH states for any (net) number of absorbed photons will lead to higher photoelectron momenta. Thus, no photoelectrons with $|p| = 0.14$ a.u. are expected in the perturbative KH picture.

[‡]The spatial part of the KH harmonics is also stretching along the polarization direction of the laser field with the increase of the intensity (see Fig. 1*D*), and this modification may contribute to the same effect.

Outlook

We have shown that the KH states become physically relevant and can be directly visualized even before the onset of the stabilization regime. They appear in the photoelectron spectra when the laser field exceeds the barrier suppression field and the oscillation amplitude α_0 is larger than the characteristic size of the system. These conditions are easily satisfied for alkaline atoms in their ground states. We expect that the formation of KH states has important implications for many strong-field phenomena. It modifies the famous recollision paradigm (26), complementing the picture of electron escape upon recollision by the possibility of populating stable closed orbits, with multiple "recollisions" leading to bound electron motion. Thus, the importance of "long" trajectories and multiple returns in the characteristic features of the photoelectron spectra associated with the so-called "channel closing" (27–29) can also be the manifestation of the KH-bound states. Bound KH states should play an important role during laser pulse filamentation in the air. Although the ionization potential of small molecules in the air is higher than that of the potassium atom considered here, even moderate laser fields with intensities approximately 10^{13} W/cm^2 suppress the potential barrier for all excited states of these molecules and lead to the formation of stable KH states. Recently it has been shown (18) that contrary to common intuition filamentation does not require strong ionization and plasma formation. The presence of bound KH states may explain this result. Even when the laser frequency is much less than the ionization potential, the electron response in such KH states is mostly determined by the linear susceptibility of the free electron, $\chi = -1/\omega^2$, providing the desired defocusing for the filament beam, yet the electron is bound and thus the plasma is not formed. The efficiency of populating the KH-bound states strongly depends on the temporal structure of the filament field. This structure is very complex; the field is strongly chirped and may have very steep rise, favorable for the efficient population of the KH states. The stability of atoms in the filament field will also strongly depend on the duration of driving laser pulses. Although we are certain that the exotic physics of the KH atom is important in understanding laser filamentation in the air, specific analysis is required to identify its exact role in this phenomenon.

Methods

Electron dynamics in the potassium atom is modeled within a single active electron approximation. The influence of the inner electrons is treated with a multiplicative effective potential. Spin-orbit coupling and other relativistic effects are neglected. One-electron potentials for the potassium atom are well-known (30–32), and can accurately reproduce its spectroscopic (30) and scattering (33) properties. The potentials (30–32) faithfully reproduce the radial nodal structure of the valence states and require dense numerical grids close to the nucleus to support the inner-shell solutions. At the same time, the strong-field ionization dynamics of the valence electron is primarily determined by outer parts of the wave function and can be accurately modeled by nodeless valence pseudo wave functions (34). We have therefore chosen to represent the potassium atom using an effective potential:

$$u_{\text{eff}}(r) = -\frac{1}{r}(1 - 7.89749e^{(-0.484234r)} + 5.7408e^{(-0.418037r)}).$$

The u_{eff} parameters were adjusted to reproduce experimental average energies of the 4*s*, 5*s*, 6*s*, 4*p*, 5*p*, 3*d*, 4*d*, 4*f*, and 5*g* multiplets, with the residual root-mean-square error of 0.07 eV. Despite the lack of the inner radial nodes, this potential yields adequate transition dipole matrix elements [e.g., $\langle 4s|z|4p_z\rangle = 3.01$ Bohr vs. 2.91 Bohr in experiment (35, 36)]. The Kramers–Henneberger potential and its harmonics (Eq. **3**) are evaluated numerically, using 1,000th-order Gauss–Legendre quadrature.

Three-dimensional stationary and time-dependent solutions of the one-electron Schrödinger equation are computed in cylindrical coordinates (37). Stationary solutions are determined using Lanczos iterations. Time-dependent solutions are obtained using real-space leap-frog propagation with time step of 0.002 a.u. on a grid extending to 700 Bohr from the origin. In all cases, uniform grid spacing of 1 a.u. was used. This grid density is sufficient to represent both the stationary and time-dependent solutions for the valence-only effective potential and laser field parameters used here. For example, the KH-state energies for $\alpha_0 = 0$ (Fig. 1*E*) agree with numerically exact results to within 0.01 eV rms error. A reflection-free absorbing boundary (38) is used at the simulation volume edges (starting at ± 635 Bohr for simulations of photoelectron spectra). The survival probability W_s is defined as the total population of the bound states after the end of the laser pulse. Because we use absorbing boundaries (for this simulation smooth boundary starts at ± 70 Bohr from the core), the norm of the wave function is not conserved: The continuum part of the wave function is absorbed. We calculate the survival probability as the total norm of the time-dependent solution of the Schrödinger equation within a 100-Bohr simulation volume, 13 cycles past the end of the pulse, when the changes in its norm become negligible. Photoelectron spectra are evaluated with Fourier–Bessel transformation of the final real-space wave functions outside the inner region after a waiting time of about 34 fs after the pulse turnoff. The inner region is defined by a real-space mask function $f_{\text{mask}}(r) = 1/(1 + \exp((r_0 - r)/d))$, with $r_0 = 100$, $d = 7$ Bohr.

Note Added in Proof. Stabilization of silver atoms in low-frequency fields has recently been analyzed in ref. 39. The same authors have also pointed out the important role of Rydberg states in nonlinear response of atoms during laser propagation in gases (40); see also ref. 41.

ACKNOWLEDGMENTS. O.S. gratefully acknowledges important and inspiring discussions with T. Baumert, who shared with O.S. his experimental data on photoelectron spectroscopy of potassium in strong laser fields. We appreciate stimulating discussions with M. Yu. Ivanov, J.-P. Wolf, J. Kasparian, P. Béjot, U. Eichmann, and W. Sandner. This research was partially supported by the Senatsausschuss Wettbewerb Leibniz prize (to O.S.). Financial support was provided by the Spanish Ministry of Education via the *Programa Nacional de Movilidad de Recursos Humanos del Plan Nacional de I-D+i 2008–2011* (to F.M.). Partial support was provided by Deutsche Forschungsgemeinschaft Grant SM292/1-2.

1. Eberly JH, Kulander KC (1993) Atomic stabilization by super-intense lasers. *Science* 262:1229–1233.
2. Pont M, Gavrila M (1990) Stabilization of atomic hydrogen in superintense, high-frequency laser fields of circular polarization. *Phys Rev Lett* 65:2362–2365.
3. Fedorov MV, Movsesyan AM (1988) Field-induced effects of narrowing of photoelectron spectra and stabilisation of Rydberg atoms. *J Phys B At Mol Opt Phys* 21:L155–L158.
4. Ivanov MYu (1988) Quasiresonant atomic ionization in a strong eletromagnetic field. *Bull Acad Sci USSR Physics Series* 52:117–121.
5. Smirnova OV, Spanner M, Ivanov M (2003) Binding bare nuclei with strong laser fields —A molecule without electrons. *Phys Rev Lett* 90:243001.
6. Henneberger W (1968) Perturbation method for atoms in intense laser fields. *Phys Rev Lett* 21:838–841.
7. Ebadi H, Keitel CH, Hatsagortsyan KZ (2011) Time analysis of above-threshold ionization in extreme-ultraviolet laser pulses. *Phys Rev A* 83:063418.
8. Forre M, Selsto S, Hansen JP, Madsen LB (2005) Exact nondipole Kramers-Henneberger form of the light-atom Hamiltonian: An application to atomic stabilization and photoelectron energy spectra. *Phys Rev Lett* 95:043601.
9. Popov AM, Tikhonov MA, Tikhonova OV, Volkova EA (2009) Comparative analysis of the strong-field ionization of a quantum system with the Coulomb and short-range potentials. *Laser Phys* 19:191–201.
10. Popov AM, Tikhonova OV, Volkova EA (1999) Applicability of the Kramers-Henneberger approximation in the theory of strong-field ionization. *J Phys B At Mol Opt Phys* 32:3331–3345.
11. Smirnova O (2000) Validity of the Kramers-Henneberger approximation. *JETP* 90:609–616.
12. Gavrila M, Simbotin I, Stroe M (2008) Low-frequency atomic stabilization and dichotomy in superintense laser fields from the high-intensity high-frequency Floquet theory. *Phys Rev A* 78:033404.
13. Volkova EA, Popov AM, Tikhonova OV (2011) *J Mod Opt* 58:1195–1205.
14. Fring A, Kostrykin V, Schrader R (1997) Ionization probabilities through ultra-intense fields in the extreme limit. *J Phys A Math Gen* 30:8599–8610.
15. Faria CFM, Fring A, Schrader R, eds. (1999) Analytical treatment of stabilization. *Laser Phys* 9:379–387.
16. Gavrila M (2002) Atomic stabilization in superintense laser fields. *J Phys B At Mol Opt Phys* 35:R147–R193.
17. Eichmann U, Nubbemeyer T, Rottke H, Sandner W (2009) Acceleration of neutral atoms in strong short-pulse laser fields. *Nature* 461:1261–1264.
18. Béjot P, et al. (2010) Higher-order Kerr terms allow ionization-free filamentation in gases. *Phys Rev Lett* 104:103903.
19. Helm H, Bjerre N, Dyer MJ, Huestis DL, Saeed M (1993) Images of photoelectrons formed in intense laser fields. *Phys Rev Lett* 70:3221–3224.

20. Wollenhaupt M, et al. (2009) Three-dimensional tomographic reconstruction of ultrashort free electron wave packets. *Appl Phys B* 95:647–651.
21. Schuricke M, et al. (2011) Strong-field ionization of lithium. *Phys Rev A* 83:023413.
22. Popov AM, Tikhonova OV, Volkova EA (2003) Strong-field atomic stabilization: numerical simulation and analytical modelling. *J Phys B At Mol Opt Phys* 36:R125–R165.
23. Sundaram B, Jensen RV (1993) "Scarring" and suppression of ionization in very intense radiation fields. *Phys Rev A* 47:1415–1430.
24. Colosimo P, et al. (2008) Scaling strong-field interactions towards the classical limit. *Nat Phys* 4:386–389.
25. Wollenhaupt M, et al. (2009) Photoelectron angular distributions from strong-field coherent electronic excitation. *Appl Phys B* 95:245–259.
26. Corkum PB (1993) Plasma perspective on strong field multiphoton ionization. *Phys Rev Lett* 71:1994–1997.
27. Borca B, Frolov MV, Manakov NL, Starace AF (2002) Threshold-related enhancement of the high-energy plateau in above-threshold detachment. *Phys Rev Lett* 88:193001.
28. Popruzhenko SV, Korneev PhA, Goreslavski SP, Becker W (2002) Laser-induced recollision phenomena: Interference resonances at channel closings. *Phys Rev Lett* 89:023001.
29. Wassaf J, Veniard V, Taieb R, Maquet A (2003) Strong field atomic ionization: Origin of high-energy structures in photoelectron spectra. *Phys Rev Lett* 90:013003.
30. Laughlin C (1992) On the accuracy of the Coulomb approximation and a model-potential method for atomic transition probabilities in alkali-like systems. *Phys Scr* 45:238–245.
31. Klapisch M (1971) A program for atomic wavefunction computations by the parametric potential method. *Comput Phys Commun* 2:239–260.
32. Magnier S, Aubert-Frécon M, Hanssen J, Le Sech C (1999) Two-electron wavefunctions for the ground state of alkali negative ions. *J Phys B At Mol Opt Phys* 32:5639–5643.
33. Lühr A, Fischer N, Saenz A (2009) Interaction of antiprotons with Rb atoms and a comparison of antiproton stopping powers of the atoms H, Li, Na, K and Rb. *Hyperfine Interact* 194:51–57.
34. Muller HG (1999) Numerical simulation of high-order above-threshold-ionization enhancement in argon. *Phys Rev A* 60:1341–1350.
35. Wang H, et al. (1997) Precise determination of the dipole matrix element and radiative lifetime of the ^{39}K 4*p* state by photoassociative spectroscopy. *Phys Rev A* 55:R1569.
36. Volz U, Schmoranzer H (1996) Precision lifetime measurements on alkali atoms and on helium by beam gas laser spectroscopy. *Phys Scr* T65:48–56.
37. Smirnova O, Patchkovskii S, Spanner M (2007) Direct XUV probing of attosecond electron recollision. *Phys Rev Lett* 98:123001.
38. Manolopoulos DE (2002) Derivation and reflection properties of a transmission-free absorbing potential. *J Chem Phys* 117:9552–9559.
39. Volkova EA, Popov AM, Tikhonova OV (2011) Ionization and stabilization of atoms in high intencity low-frequency field. *Zh Eksp Teor Fiz* 140:450–465.
40. Volkova EA, Popov AM, Tikhonova OV (2011) Non-linear polarization response of an atomic gas medium to the intense femtosecond laser pulse. *Pis'ma Zh Eksp Teor Fiz* 94, in press.
41. Popov AM (2011) Book of abstracts, talk 5.2.4. *Proceedings of the 20th International Laser Physics Workshop (LPHYS'11, Sarajevo, Bosnia and Herzegovina)*, http://www.lasphys.com/workshops/lasphys11/program.pdf.